ACS Medicinal Chemistry Letters

Letter

Strategic Incorporation of Polarity in Heme-Displacing Inhibitors of Indoleamine-2,3-dioxygenase-1 (IDO1)

Catherine White, Meredeth A. McGowan, Hua Zhou, Nunzio Sciammetta, Xavier Fradera, Jongwon Lim, Elizabeth M Joshi, Christine Andrews, Elliott B. Nickbarg, Phillip Cowley, Sarah Trewick, Martin Augustin, Konstanze von König, Charles A Lesburg, Karin Otte, Ian Knemeyer, Hyun Woo, Wensheng Yu, Mangeng Cheng, Peter Spacciapoli, Prasanthi Geda, Xuelei Song, Nadya Smotrov, Patrick Curran, Mee Ra Heo, Pravien Abeywickrema, J. Richard Miller, David Jonathan Bennett, and Yongxin Han

ACS Med. Chem. Lett., **Just Accepted Manuscript** • DOI: 10.1021/acsmedchemlett.0c00010 • Publication Date (Web): 10 Mar 2020

Just Accepted

Strategic Incorporation of Polarity in Heme-Displacing Inhibitors of Indoleamine-2,3-dioxygenase-1 (IDO1)

Catherine White*[Ω], Meredeth A. McGowan*[Ω], Hua Zhou[Ω], Nunzio Sciammetta[Ω], Xavier Fradera[Δ], Jongwon Lim[Ω], Elizabeth M. Joshi[e], Christine Andrews[∂], Elliott B. Nickbarg[∂], Phillip Cowley[†], Sarah Trewick[†], Martin Augustin[Σ], Konstanze von Köenig[Σ], Charles A. Lesburg[Δ], Karin Otte[e], Ian Knemeyer[e], Hyun Woo[e], Wensheng Yu[Ω], Mangeng Cheng[Π], Peter Spacciapoli[Π∞], Prasanthi Geda[Π], Xuelei Song[Π], Nadya Smotrov[Π], Patrick Curran[Π], Mee Ra Heo[Π], Pravien Abeywickrema[Δ†], J. Richard Miller[Π], David Jonathan Bennett[Ω], and Yongxin Han[Ω]

[Ω]Department of Chemistry, [Δ]Computational and Structural Chemistry, [Π]In Vitro Pharmacology, [e]Pharmacokinetics, Pharmacodynamics & Drug Metabolism, [∂]Automated Ligand Identification System

Merck & Co., Inc., 33 Avenue Louis Pasteur, Boston, Massachusetts 02115, United States

[Σ]Proteros biostructures GmbH. 82152 Martinsried, Germany

[∞]Deceased April 15, 2019

KEYWORDS: IDO1, heme displacer, oxetane, AlogP$_{98}$

ABSTRACT: Indoleamine-2,3-dioxygenase-1 (IDO1) has emerged as a target of significant interest to the field of cancer immunotherapy, as the upregulation of IDO1 in certain cancers has been linked to host immune evasion and poor prognosis for patients. In particular, IDO1 inhibition is of interest as a combination therapy with immune checkpoint inhibition. Through an Automated Ligand Identification System (ALIS) screen, a diamide class of compounds was identified as a promising lead for the inhibition of IDO1. While hit **1** possessed attractive cell-based potency, it suffered from a significant right-shift in a whole blood assay, poor solubility, and poor pharmacokinetic properties. Through a physicochemical property-based approach, including a focus on lowering AlogP$_{98}$ *via* the strategic introduction of polar substitution, compound **13** was identified bearing a pyridyl oxetane core. Compound **13** demonstrated improved whole blood potency and solubility, and an improved pharmacokinetic profile resulting in a low predicted human dose.

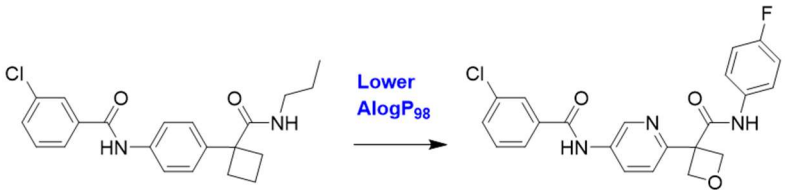

	1	13
IDO1 HeLa IC_{50}	9 nM	3.2 nM
IDO1 hWB_u IC_{50}	22 nM	0.6 nM
$AlogP_{98}$	4.4	3.1
FASSIF Soly (μM) pH 6.5	58	170
Rat *in vivo* Cl_{int} (ml/min/kg), Vd_u (L/kg), MRT(h)	>Qhep, 180, 0.7	590, 99, 3.2

Indoleamine-2,3-dioxygenase-1 (IDO1) is a heme-containing enzyme which catalyzes the oxidation of essential amino acid tryptophan (Trp) as the first and rate-limiting step of the kynurenine pathway. Both depletion of Trp and the production of kynurenine and other pathway metabolites contribute to local immunosuppression, manipulating multiple components of the innate and adaptive immune system including CD8+ T cells, effector T (T_{eff}) cells, and natural killer (NK) cells.[1-4] Many human tumors have been shown to exploit this pathway by upregulating the expression of IDO1,[5-7] and an increased level of IDO1 expression in tumor cells is correlated with poor prognosis in several tumor types.[8, 9] Given its role in contributing to immune escape, IDO1 has emerged as an important therapeutic target in cancer immunotherapy.[10, 11] Initial proof of concept for IDO1 inhibition in the clinic was established with epacadostat[12, 13] in combination with anti-PD-1 (programmed cell death protein 1) antibodies.[14] The recent failure of this combination to show improved efficacy over anti-PD-1 monotherapy in a phase 3 study (ECHO-

301/KEYNOTE-252) has prompted speculation that epacadostat may have failed to achieve sufficient target engagement in the tumor microenvironment.[15] Thus, the investigation of IDO1 inhibition continues in the clinic,[16] and it remains highly desirable to discover new highly potent and selective IDO1 inhibitors which allow for achievement of higher levels of target engagement.

Over the past several years, there have been multiple reports describing alternative binding modes and mechanisms of action for IDO1-selective inhibitory small molecules. Epacadostat inhibits IDO1 *via* a competitive binding mechanism, occupying the Trp binding site and coordinating to the heme-bound iron, while an uncompetitive inhibitor such as mitomycin C occupies an allosteric site located on the opposite side of the heme in the protein.[17] Additionally, it has recently been demonstrated that the heme cofactor is labile and can be displaced entirely, allowing for inhibitors to bind to the apoenzyme and thus prevent heme from re-binding.[18] In fact, it has been shown that a majority of IDO1 present in the cell is in its apo form. This class of inhibitors are therefore particularly effective in a cellular setting, but require extended incubation times and elevated temperatures to effect inhibition in a functional enzymatic assay where the heme is pre-incorporated.

As part of our efforts towards identifying a small molecule inhibitor of IDO1, we performed an affinity-based primary screen of 260,000 compounds against IDO1 using Automated Ligand Identification System (ALIS) technology. This screening method relies on identification of small molecules which bind to a target of interest *via* a mass-spectrometry-based detection using pooled libraries of compounds with known and distinct masses.[19-21,22] Significantly, the protein employed for this screen was found to have achieved between 80% and 90% heme incorporation during its biosynthesis, and thus both apo and heme-bound forms of the protein were present (see Supporting Information for protein preparation protocol). From this screening campaign, diamide **1** was identified as a promising hit, displaying potent activity in a HeLa cell-based assay measuring production of the product of IDO1-mediated tryptophan oxidation, N-formylkynurenine (Hela IC50 = 9 nM, see Supporting Information for assay details). Interestingly, **1** was inactive in a biochemical IDO1 inhibition assay, prompting speculation that **1** acts as a heme-displacing IDO1 inhibitor as described above.[23] A high-resolution co-crystal structure was obtained with apo IDO1 and compound **1** (Figure 1; PDB [protein database] entry 6V52), which confirmed that **1** binds in such a manner that it occupies the binding site of the absent heme cofactor. This binding mode is further illustrated by an overlay[24] of the crystal structure of **1** with a recently disclosed heme-displacing inhibitor (compound **2**, Figure 2)[18,25] and heme (PDB entry 6e40).[26] The structure also reveals that **1** is anchored to the protein *via* a network of hydrogen bonds, extending from the propyl-substituted amide directly to Ser167 and (*via* water) His346, as well as two water-mediated hydrogen bonds from the aryl amide to Ser267 and Arg343. The aryl amide extends below the plane of the absent heme to occupy a largely hydrophobic pocket (which we termed the "C" pocket). The *n*-propyl amide substituent extends into and partially filled a hydrophobic pocket above the absent heme (termed the "A" pocket),[17] which in the case of compound **2** is occupied by an aryl substituent.

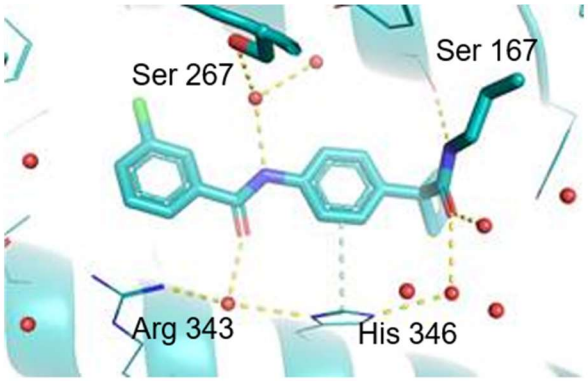

Figure 1. Hydrogen bonding network made by compound **1** in the heme-binding region.

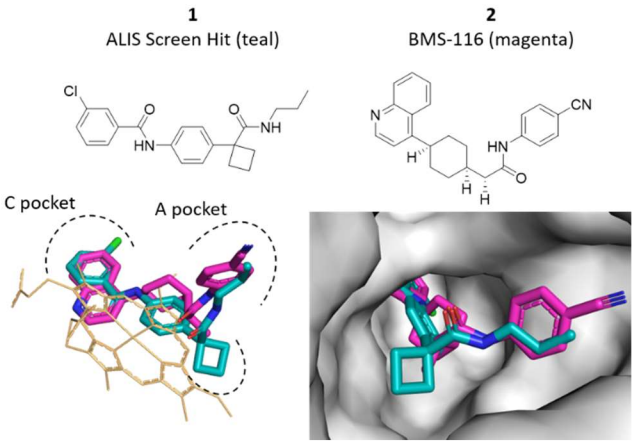

Figure 2. Overlay of compounds **1** (teal) and **2** (gray) with the heme binding location (yellow). The A- and C-pockets are indicated. Residues omitted for clarity.

As an initial lead, compound **1** displayed potent suppression of N-formylkynurenine production in HeLa cells, coupled with promising unbound potency (22 nM) as assessed in a whole blood assay measuring kynurenine production and corrected for human plasma protein binding[27] (Table 1). However, compound **1** suffered from high turnover in *in vitro* microsome and hepatocyte systems,[28] and a short mean residence time (MRT) when dosed *in vivo*. In light of this data, the predicted once-daily (QD, or quaque die) human dose for compound **1**, as estimated by allometric scaling based on rat pharmacokinetic parameters,[29] was in excess of 10g QD (See Supporting Information for details).

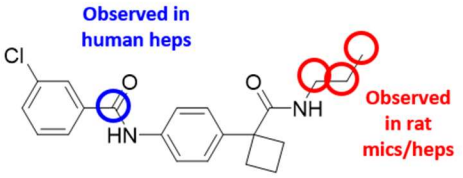

	1
IDO1 Hela IC_{50}	9.2 nM
IDO1 hWB_u IC_{50}	22 nM
Human/Rat Hepatocytes $Cl_{int,u}$ (mL/min/kg)	870 / 7200
Rat PK (Cl, V, MRT, Fu%)	110 ml/min/kg, 4.9 L/kg, 0.7 h, 2.6%
Rat Cl_u Measured	4100

Figure 3. *In vitro* metabolic profile of compound **1**.

Metabolic identification (MetID) assessments were conducted on compound **1** to identify primary metabolic liabilities, and the results indicated that initial oxidative metabolism occurred on the *n*-propyl group in rat and human microsomes, and additionally that the aryl amide bond was readily cleaved in human hepatocytes (Figure 3). To address the propyl group oxidation, and guided by the crystal structure which suggested an opportunity to further optimize van der Waals interactions in the A-pocket, compound **3** was synthesized which incorporated a fluorophenyl amide. A significant increase in both HeLa and whole blood potency was observed with compound **3** as compared to **1**, however the human hepatocyte turnover remained high. In addition, a significant drop in solubility was observed, which was hypothesized to lead to complications with respect to formulation and dosing.

As outlined above, it is of significant importance that the next generation of IDO1 inhibitors are capable of achieving high levels of target engagement in clinical trials. As such, our goal was to identify a compound predicted to require a low dose to achieve excellent levels of target engagement in humans, which we defined as the ability to achieve greater than 75% inhibition (or IC_{75} as measured in the whole blood assay) over a 24h period. While highly potent, compound **3** is also highly lipophilic ($AlogP_{98}$ = 5.3), [30] residing outside of traditional drug-like space.[31, 32] This high lipophilicity is likely contributing to poor solubility and *in vitro* hepatocyte stability. It has been demonstrated in the medicinal chemistry literature that modulation of physicochemical properties such as $AlogP_{98}$ can have a dramatic effect on pharmacokinetic parameters.[33, 34] Therefore, moving forward, one of our strategies for the optimization of this series of IDO1 inhibitors was to seek opportunities to introduce polarity to aspirationally improve both metabolic stability as well as compound solubility.

Given the modular nature of the hit scaffold, with amide bonds amenable to structure-activity relationship (SAR) exploration *via* amide library synthesis, initial efforts focused on the rapid exploration of alternative substitution in the A- and C- pockets in the background of compound **1** and with a focus on the addition of polar functionality. Selected examples of this exploration are depicted in Table **1** (compounds **4-8**). As many of the compounds in this series are highly protein-bound in human plasma, it was useful to compare unbound potency values as measured in the human whole blood assay to decouple the plasma protein binding and target interaction components. Gratifyingly, the introduction of a more polar pyran substituent, for example, resulted in greater *in vitro* stability (compound **4**). Unfortunately, most polar substitution was not tolerated in either of the largely hydrophobic pockets in terms of potency, and in this sense only minor changes were tolerated (compound **6**). A notable exception was compound **5**, which featured a 2-substituted pyridine. However, while this compound possessed favorable solubility, it also carried a significant hERG (human Ether-a-go-go-Related Gene) liability (420 nM in a hERG binding assay) and was not pursued further.

Having concluded from these initial explorations that substituents projecting into the A- and C-pockets must remain hydrophobic, attention was turned towards exploration of polar functionality in the central core of the hit structure. In the context of the fluorophenyl group at the R^1 position, a pyridine was tolerated in place of the central phenyl ring (compound **9**), resulting in a compound with comparable HeLa potency and 6-fold shifted unbound hWB (human whole blood) potency. Additionally, **9** displayed improved kinetic solubility while maintaining hepatocyte stability with respect to **3**. Interestingly, pyrimidine substitution (**10**) did not improve solubility, despite its lowered $AlogP_{98}$ value, and furthermore was not tolerated in terms of potency.

In addition to the phenyl portion of the core, the cyclobutane offered an opportunity for the introduction of polar substituents. We hypothesized that an oxetane, as a polar, metabolically robust cyclobutane alternative,[35-38] would significantly lower the compound lipophilicity with minimal effect on compound binding. Indeed, introduction of an oxetane dramatically lowered the $AlogP_{98}$ to 3.8 (compound **11**), and a corresponding improvement in hepatocyte stability was observed as compared to **3**. Moreover, **11** did not suffer from any potency loss as a result of the introduction of the oxetane. To further investigate polar substitution in the cyclobutane region, compound **12** was synthesized featuring a hydroxycyclobutane. While compound **12** also displayed improved *in vitro* stability as compared to **3**, the hydroxy substitution was not tolerated in the binding pocket and both HeLa and hWB potencies were significantly shifted. Finally, we sought to combine the successful polar core substitutions into a single analog featuring a 2-pyridyl oxetane (compound **13**). Compound **13** displayed an excellent unbound hWB potency of 0.6 nM, and dramatically improved FaSSIF (fasted simulated small intestinal fluid) solubility (170 μM) (see Supporting Information for experimental procedure to determine FaSSIF solubility). Moreover, compound **13** possessed excellent stability in both human and rat hepatocytes, as it was completely stable over the course of the experiment.

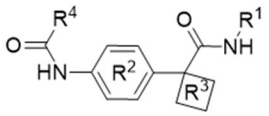

R^1	R^2	R^3	R^4	Cmpd	HeLa IC_{50} (nM)[a]	hWB_u IC_{50} (nM)[a]	AlogP98	FaSSIF Soly (μM) pH 6.5	$C_{lint,u}$ (Hep) H/R
			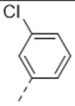	1	9.2	22	4.4	58	870 / 7200
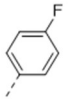	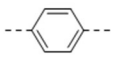		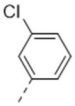	3	1.7	0.05	5.3	2	2000 / 2000
	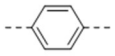		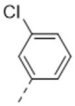	4	19	49	3.3	11	390 / 1700
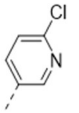	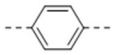		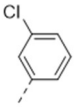	5	3.6	0.04	4.8	81	1900 / 500
	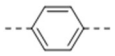		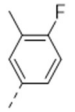	6	8.3	3.0	4.4	23	560 / 6200
	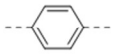			7	3800	--	2.3	140	--
				8	>10000 (n=1)	--	2.3	160	--
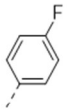	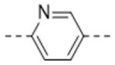		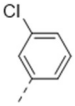	9	2.7	0.3	4.7	83	1300 / 830
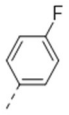	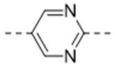		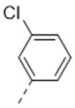	10	17	--	3.6	14	--
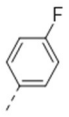	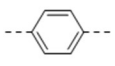			11	2.1	0.09	3.8	76	420 / 250
				12	32	14	4.0	180	350 / <280
				13	3.2	0.6	3.1	170	<44/<84

Table 1: SAR exploration of the diamide scaffold.

[a]Reported assay data is the geometric mean of n = 2 or greater.

Cmpd	AlogP$_{98}$	Rat *in vivo* Cl$_{int}$ (ml/min/kg), Vdu (L/kg), MRT(h)	Predicted Human QD Dose[d]
1	4.4	>Q$_{hep}$[c], 180, 0.7[a]	>10 g
3	5.3	6000, 1100, 4.3[a]	16 mg
9	4.7	45000, 2200, 5.0[b]	280 mg
11	3.8	1600, 420, 4.8[a]	6 mg
13	3.1	590, 99, 3.2[a]	26 mg

Table 2: Pharmacokinetic parameters on selected compounds

[a]Protocol Rat Cassette: route IV; Dose 0.05 mg/kg; Dose Vol 1 ml/kg; formulation DMSO/PEG400/H_2O-20/60/20; Fasted. [b]Protocol Rat 2x2: route IV; Dose 0.5 mg/kg; Dose Vol 1 ml/kg; formulation DMSO/PEG400/H_2O-20/60/20; route PO; Dose 1 mg/kg; Dose Vol 2 ml/kg; formulation DMSO/PEG400/H_2O-20/60/20. [c]Reported assay data is the geometric mean of n = 2 or greater. [d]Based on rat allometry

Selected compounds depicted in Table 1 were further profiled *in vivo* and evaluated for a predicted human dose, as depicted in Table 2. Initial hit compound **1**, which was demonstrated above to be readily oxidized at the propyl group, was also rapidly cleared in a rat cassette and displayed plasma clearance greater than rat hepatic blood flow. Replacing the propyl group with the fluorophenyl group (compound **3**) resulted in a dramatic improvement in MRT and a low allometry-predicted dose. However, as mentioned above, the compound was unattractive due to poor solubility. The introduction of a pyridine (compound **9**) maintained the favorable rat MRT as compared to compound **3**, however the predicted dose was shifted due to a six-fold decrease in intrinsic whole blood potency. The introduction of the oxetane into the core (**11**) also served to maintain a favorable rat MRT and similar intrinsic whole blood potency, however **11** was significantly less stable in human hepatocytes as compared to rat, and for this reason there was uncertainty around the allometry-predicted dose (see Supporting Information). Finally, pyridyl oxetane compound **13** displayed a favorable rat MRT of 3.2h, and moreover was more stable both as reflected by the *in vivo* Cl$_{int}$[39] (intrinsic clearance) and *in vitro* hepatocyte stability across species as mentioned above. This stability, favorable rat PK (pharmacokinetics), and improved solubility, combined with excellent potency, resulted in a human QD dose prediction of 26 mg (Table 2).

To further assess the suitability of compound **13** as a lead compound, **13** was profiled in a panel of off-target assays. Over the 108 protein targets evaluated, there were no targets for which the IC50 of compound **13** was <10 μM (see Supporting Information). It is worthwhile to note that compound **9** was also evaluated in the same panel, and was found to hit 4 targets below the 10 μM threshold. This improved off-target profile may be at least partially attributed to a lower AlogP$_{98}$, a phenomenon that has been noted in numerous discovery efforts reported in the literature.[40-43] Thus, pyridyl oxetane **13** represented an attractive compound for further development as a low-dose QD inhibitor of IDO1.

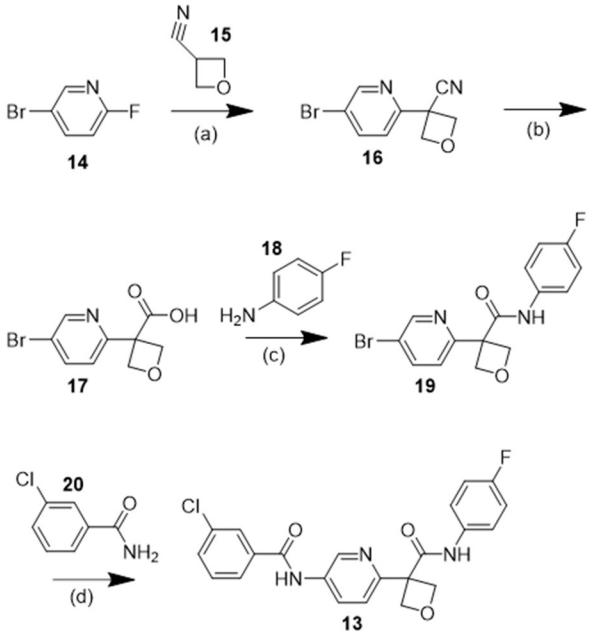

Scheme 1. Synthesis of **13**. (a) KHMDS, toluene, 0°C, 47% yield; (b) NaOH, ethanol, water, 80 °C, 90% yield; (c) HATU, DIEA, DMF, room temperature, 86% yield; (d) Cs_2CO_3, (1*S*,2*S*)-*N*1,*N*2-dimethylcyclohexane-1,2-diamine, dioxane, Cu(I)I, 110 °C, 74.5% yield.

Despite its utility and metabolic stability as demonstrated above, the pyridyl oxetane substitution pattern leveraged in lead compound **13** was not previously reported in the literature. To rapidly access this core, it was found that commercially available oxetane-3-carbonitrile (**15**) could be directly deprotonated through the use of potassium bis(trimethylsilyl)amide (KHMDS) at reduced temperatures, and that this nucleophile could be readily added to 5-bromo-2-fluoropyridine (**14**) to provide 3-(5-bromopyridin-2-yl)oxetane-3-carbonitrile (**16**) in reasonable yields (Scheme 1).[44] The nitrile could then be hydrolyzed to the carboxylic acid (**17**), after which, for the purposes of this series, could engage in an amide coupling to provide **19**. Compound **19** was then subjected to copper-catalyzed C-N coupling conditions to provide lead compound **13**.

In conclusion, an affinity-based screening method (ALIS) led to the rapid identification of a diamide-containing IDO1 heme-displacing inhibitor with promising cell-

based potency, but which suffered from high clearance and a significant whole blood shift. Through a crystal structure-inspired optimization of A-pocket substitution, it was discovered that a phenyl group significantly enhanced potency. A subsequent physicochemical property-led investigation of SAR (structure–activity relationship) led to the discovery that a strategic incorporation of polarity into the core of the structure was tolerated in terms of potency and greatly enhanced the pharmacokinetic profile of the resulting compounds. These investigations resulted in a lead compound with an excellent predicted human dose and a favorable off-target profile for further development.

ASSOCIATED CONTENT

Supporting Information

The Supporting Information is available free of charge on the ACS Publications website.

The crystal structure of human IDO1 in complex with compound **1** has been deposited at the PDB (http://www.rcsb.org) with accession code 6V52.

AUTHOR INFORMATION

Corresponding Author

*E-mail: catherine_white@merck.com. Phone: 617-992-2105.
*E-mail: meredeth.mcgowan@merck.com. Phone: 617- 992-3252.

Present Addresses

†Phillip Cowley (PMC Discovery Limited, Edinburgh, United Kingdom), †Sarah Trewick (Edinburgh Innovations, Edinburgh, United Kingdom), †Pravien Abeywickrema (The Janssen Pharmaceutical Companies of Johnson and Johnson, Pennsylvania), †Prasanthi Geda (AbbVie, Illinois)

Author Contributions

The manuscript was written through contributions of all authors. All authors have given approval to the final version of the manuscript.

ACKNOWLEDGMENT

Chad Chamberlin, Omar Mabrouk, Patrick Curran, Matt Richards, and Peter Saradjian for their contributions to the ALIS screen. Lisa Nogle, David Smith, and Mark Pietrafitta for their contributions as members of the Separation Sciences Team. Adam Beard for his contributions to high quality purity determination.

ABBREVIATIONS

ALIS, Automated Ligand Identification System; IDO1, Indoleamine-2,3-dioxygenase-1; hWBu, human whole blood, unbound potency; FaSSIF, fasted simulated small intestinal fluid; Clint, intrinsic clearance; Vd_u Volume of distribution unbound; MRT, Mean residence time; PD-1, Programmed cell death protein 1; PDB, protein database; QD, quaque die; MetID, Metabolic identification; hERG, human Ether-a-go-go-Related Gene; KHMDS, Potassium bis(trimethylsilyl)amide; C-N couplings, carbon-nitrogen couplings; NaOH, sodium hydroxide; HATU, 1-[Bis(dimethylamino)methylene]-1H-1,2,3-triazolo[4,5-b]pyridinium 3-oxide hexafluorophosphate; DIEA, *N,N*-Diisopropylethylamine; DMF, dimethylformamide; Cs2CO3, cesium carbonate; Cu(I)I, Copper(I) iodide; PK, pharmacokinetics; SAR, structure–activity relationship.

REFERENCES

1. Fallarino, F.; Grohmann, U.; You, S.; McGrath, B. C.; Cavener, D. R.; Vacca, C.; Orabona, C.; Bianchi, R.; Belladonna, M. L.; Volpi, C.; Santamaria, P.; Fioretti, M. C.; Puccetti, P., The combined effects of tryptophan starvation and tryptophan catabolites down-regulate T cell receptor zeta-chain and induce a regulatory phenotype in naive T cells. *J Immunol* **2006,** *176* (11), 6752-61.
2. Prendergast, G. C.; Malachowski, W. P.; DuHadaway, J. B.; Muller, A. J., Discovery of IDO1 Inhibitors: From Bench to Bedside. *Cancer Res* **2017,** *77* (24), 6795-6811.
3. Stone, T. W.; Stoy, N.; Darlington, L. G., An expanding range of targets for kynurenine metabolites of tryptophan. *Trends Pharmacol Sci* **2013,** *34* (2), 136-43.
4. Munn, D. H.; Mellor, A. L., Indoleamine 2,3 dioxygenase and metabolic control of immune responses. *Trends Immunol* **2013,** *34* (3), 137-43.
5. Munn, D. H.; Mellor, A. L., Indoleamine 2,3-dioxygenase and tumor-induced tolerance. *J Clin Invest* **2007,** *117* (5), 1147-54.
6. Litzenburger, U. M.; Opitz, C. A.; Sahm, F.; Rauschenbach, K. J.; Trump, S.; Winter, M.; Ott, M.; Ochs, K.; Lutz, C.; Liu, X. D.; Anastasov, N.; Lehmann, I.; Hofer, T.; von Deimling, A.; Wick, W.; Platten, M., Constitutive IDO expression in human cancer is sustained by an autocrine signaling loop involving IL-6, STAT3 and the AHR. *Oncotarget* **2014,** *5* (4), 1038-1051.
7. Platten, M.; Wick, W.; Van den Eynde, B. J., Tryptophan Catabolism in Cancer: Beyond IDO and Tryptophan Depletion. *Cancer Research* **2012,** *72* (21), 5435-5440.
8. Yu, C. P.; Fu, S. F.; Xuan-Chen; Jing-Ye; Yuan-Ye; Kong, L. D.; Zhu, Z. M., The Clinicopathological and Prognostic Significance of IDO1 Expression in Human Solid Tumors: Evidence from a Systematic Review and Meta-Analysis. *Cell Physiol Biochem* **2018,** *49* (1), 134-143.
9. Godin-Ethier, J.; Hanafi, L.-A.; Piccirillo, C. A.; Lapointe, R., Indoleamine 2,3-Dioxygenase Expression in Human Cancers: Clinical and Immunologic Perspectives. *Clin Cancer Res* **2011,** *17* (22), 6985-6991.
10. Rohrig, U. F.; Majjigapu, S. R.; Vogel, P.; Zoete, V.; Michiein, O., Challenges in the Discovery of Indoleamine 2,3-Dioxygenase 1 (IDO1) Inhibitors. *J Med Chem* **2015,** *58* (24), 9421-9437.
11. Platten, M.; Doeberitz, N. V.; Oezen, I.; Wick, W.; Ochs, K., Cancer immunotherapy by targeting IDO1/TDO and their downstream effectors. *Front Immunol* **2015,** *5*.
12. Yue, E. W.; Douty, B.; Wayland, B.; Bower, M.; Liu, X. D.; Leffet, L.; Wang, Q.; Bowman, K. J.; Hansbury, M. J.; Liu, C. N.; Wei, M.; Li, Y. L.; Wynn, R.; Burn, T. C.; Koblish, H. K.; Fridman, J. S.; Metcalf, B.; Scherle, P. A.; Combs, A. P., Discovery of Potent Competitive Inhibitors of Indoleamine

2,3-Dioxygenase with in Vivo Pharmacodynamic Activity and Efficacy in a Mouse Melanoma Model. *J Med Chem* **2009,** *52* (23), 7364-7367.

13. Koblish, H. K.; Hansbury, M. J.; Bowman, K. J.; Yang, G. J.; Neilan, C. L.; Haley, P. J.; Burn, T. C.; Waeltz, P.; Sparks, R. B.; Yue, E. W.; Combs, A. P.; Scherle, P. A.; Vaddi, K.; Fridman, J. S., Hydroxyamidine Inhibitors of Indoleamine-2,3-dioxygenase Potently Suppress Systemic Tryptophan Catabolism and the Growth of IDO-Expressing Tumors. *Mol Cancer Ther* **2010,** *9* (2), 489-498.

14. Beatty, G. L.; O'Dwyer, P. J.; Clark, J.; Shi, J. G.; Bowman, K. J.; Scherle, P. A.; Newton, R. C.; Schaub, R.; Maleski, J.; Leopold, L.; Gajewski, T. F., First-in-Human Phase I Study of the Oral Inhibitor of Indoleamine 2,3-Dioxygenase-1 Epacadostat (INCB024360) in Patients with Advanced Solid Malignancies. *Clin Cancer Res* **2017,** *23* (13), 3269-3276.

15. Muller, A. J.; Manfredi, M. G.; Zakharia, Y.; Prendergast, G. C. J. S. i. I., Inhibiting IDO pathways to treat cancer: lessons from the ECHO-301 trial and beyond. *Semin Immunopathol* **2019,** *41* (1), 41-48.

16. Komiya, T.; Huang, C. H., Updates in the Clinical Development of Epacadostat and Other Indoleamine 2,3-Dioxygenase 1 Inhibitors (IDO1) for Human Cancers. *Front Oncol* **2018,** *8*.

17. Lewis-Ballester, A.; Pham, K. N.; Batabyal, D.; Karkashon, S.; Bonanno, J. B.; Poulos, T. L.; Yeh, S. R., Structural insights into substrate and inhibitor binding sites in human indoleamine 2,3-dioxygenase 1. *Nat Commun* **2017,** *8*.

18. Nelp, M. T.; Kates, P. A.; Hunt, J. T.; Newitt, J. A.; Balog, A.; Maley, D.; Zhu, X.; Abell, L.; Allentoff, A.; Borzilleri, R.; Lewis, H. A.; Lin, Z. Y.; Seitz, S. P.; Yan, C. H.; Groves, J. T., Immune-modulating enzyme indoleamine 2,3-dioxygenase is effectively inhibited by targeting its apo-form. *P Natl Acad Sci USA* **2018,** *115* (13), 3249-3254.

19. Kutilek, V. D.; Andrews, C. L.; Richards, M. P.; Xu, Z. W.; Sun, T. X.; Chen, Y. P.; Hashke, A.; Smotrov, N.; Fernandez, R.; Nickbarg, E. B.; Chamberlin, C.; Sauvagnat, B.; Curran, P. J.; Boinay, R.; Saradjian, P.; Allen, S. J.; Byrne, N.; Elsen, N. L.; Ford, R. E.; Hall, D. L.; Kornienko, M.; Rickert, K. W.; Sharma, S.; Shipman, J. M.; Lumb, K. J.; Coleman, K.; Dandliker, P. J.; Kariv, I.; Beutel, B., Integration of Affinity Selection-Mass Spectrometry and Functional Cell-Based Assays to Rapidly Triage Druggable Target Space within the NF-B Pathway. *J Biomol Screen* **2016,** *21* (6), 608-619.

20. Annis, D. A.; Athanasopoulos, J.; Curran, P. J.; Felsch, J. S.; Kalghatgi, K.; Lee, W. H.; Nash, H. M.; Orminati, J. P. A.; Rosner, K. E.; Shipps, G. W.; Thaddupathy, G. R. A.; Tyler, A. N.; Vilenchik, L.; Wagner, C. R.; Wintner, E. A., An affinity selection-mass spectrometry method for the identification of small molecule ligands from self-encoded combinatorial libraries - Discovery of a novel antagonist of E-coli dihydrofolate reductase. *Int J Mass Spectrom* **2004,** *238* (2), 77-83.

21. Annis, D. A.; Nickbarg, E.; Yang, X.; Ziebell, M. R.; Whitehurst, C. E., Affinity selection-mass spectrometry screening techniques for small molecule drug discovery. *Curr Opin Chem Biol* **2007,** *11* (5), 518-526.

22. Andrews, C. L., Ziebell, M. R., Nickbarg, E., & Yang, X. (2012). Mass Spectrometry-Based Screening and Characterization of Protein–Ligand Complexes in Drug Discovery. In M. L. Gross, G. Chen, & B. N. Pramanik (Eds.), Protein and Peptide Mass Spectrometry in Drug Discovery (pp. 255-286). Hoboken, NJ: John Wiley & Sons, Inc.

23. See Supporting Information for IDO1 biochemical and HeLa assay protocols.

24. Overlays were rendered in The PyMOL Molecular Graphics System, Version 2.1.1 Schrödinger, LLC

25. Beck, H.P et al(2016) Patent Cooperation Treaty Int Appl WO 2016073770.

26. Luo, S.; Xu, K.; Xiang, S.; Chen, J.; Chen, C.; Guo, C.; Tong, Y.; Tong, L., High-resolution structures of inhibitor complexes of human indoleamine 2,3-dioxygenase 1 in a new crystal form. *Acta Crystallogr F Struct Biol Commun* **2018,** *74* (Pt 11), 717-724.

27. The value for unbound human whole blood IC50 was obatained using the following equation: hWBu = (measured IDO1 hWB IC50) * (Human fu plasma)

28. Please see the Supporting Information for experimental details regarding *in vitro* compound stability in hepatocyte and microsome systems.

29. Hosea, N. A.; Collard, W. T.; Cole, S.; Maurer, T. S.; Fang, R. X.; Jones, H.; Kakar, S. M.; Nakai, Y.; Smith, B. J.; Webster, R.; Beaumont, K., Prediction of human pharmacokinetics from preclinical information: comparative accuracy of quantitative prediction approaches. J *Clin Pharmacol* **2009,** *49* (5), 513-33.

30. Ghose, A. K.; Viswanadhan, V. N.; Wendoloski, J. J., Prediction of hydrophobic (lipophilic) properties of small organic molecules using fragmental methods: An analysis of ALOGP and CLOGP methods. J *Phys Chem A* **1998,** *102* (21), 3762-3772.

31. Lipinski, C. A., Drug-like properties and the causes of poor solubility and poor permeability. J *Pharmacol Toxicol Methods* **2000,** *44* (1), 235-49.

32. Lipinski, C. A.; Lombardo, F.; Dominy, B. W.; Feeney, P. J., Experimental and computational approaches to estimate solubility and permeability in drug discovery and development settings. A*dv Drug Deliv Rev* **2001,** *46* (1-3), 3-26.

33. Lazerwith, S. E.; Bahador, G.; Canales, E.; Cheng, G. F.; Chong, L.; Clarke, M. O.; Doerffler, E.; Eisenberg, E. J.; Hayes, J.; Lu, B.; Liu, Q.; Matles, M.; Mertzman, M.; Mitchell, M. L.; Morganelli, P.; Murray, B. P.; Robinson, M.; Strickley, R. G.; Tessler, M.; Tirunagari, N.; Wang, J. H.; Wang, Y. J.; Zhang, J. R.; Zheng, X. B.; Zhong, W. D.; Watkins, W. J., Optimization of Pharmacokinetics through Manipulation of Physicochemical Properties in a Series of HCV Inhibitors. A*cs Med Chem Lett* **2011,** *2* (10), 715-719.

34. Meanwell, N. A., Improving Drug Design: An Update on Recent Applications of Efficiency Metrics, Strategies for Replacing Problematic Elements, and Compounds in Nontraditional Drug Space. *Chem Res Toxicol* **2016,** *29* (4), 564-616.

35. Wuitschik, G.; Rogers-Evans, M.; Muller, K.; Fischer, H.; Wagner, B.; Schuler, F.; Polonchuk, L.; Carreira, E. M., Oxetanes as promising modules in drug discovery. A*ngew Chem Int Edit* **2006,** *45* (46), 7736-7739.

36. Burkhard, J. A.; Wuitschik, G.; Rogers-Evans, M.; Muller, K.; Carreira, E. M., Oxetanes as versatile elements in drug discovery and synthesis. A*ngew Chem Int Ed Engl* **2010,** *49* (48), 9052-67.

37. Stepan, A. F.; Karki, K.; McDonald, W. S.; Dorff, P. H.; Dutra, J. K.; DiRico, K. J.; Won, A.; Subramanyam, C.; Efremov, I. V.; O'Donnell, C. J.; Nolan, C. E.; Becker, S. L.; Pustilnik, L. R.; Sneed, B.; Sun, H.; Lu, Y. S.; Robshaw, A. E.; Riddell, D.; O'Sullivan, T. J.; Sibley, E.; Capetta, S.; Atchison, K.; Hallgren, A. J.; Miller, E.; Wood, A.; Obach, R. S., Metabolism-Directed Design of Oxetane-Containing Arylsulfonamide Derivatives as gamma-Secretase Inhibitors. J *Med Chem* **2011,** 54 (22), 7772-7783.

38. Toselli, F.; Fredenwall, M.; Svensson, P.; Li, X. Q.; Johansson, A.; Weidolf, L.; Hayes, M. A., Hip To Be Square: Oxetanes as Design Elements To Alter Metabolic Pathways. J *Med Chem* **2019,** 62 (16), 7383-7399.

39. The value for rat in vivo Clint was obtained using the following equation: Rat in vivo Clint = [Qh*Clp] / [fu,p*(Qh-(Clp/B:P))]

40. Koslov-Davino, E.; Wang, X.; Schroeter, T., Target promiscuity and physicochemical properties contribute to pharmacologically induced ER-stress. T*oxicol In Vitro* **2013,** 27 (1), 204-10.

41. Peters, J. U.; Schnider, P.; Mattei, P.; Kansy, M., Pharmacological promiscuity: dependence on compound properties and target specificity in a set of recent Roche compounds. Ch*emMedChem* **2009, 4** (4), 680-6.

42. Hughes, J. D.; Blagg, J.; Price, D. A.; Bailey, S.; Decrescenzo, G. A.; Devraj, R. V.; Ellsworth, E.; Fobian, Y. M.; Gibbs, M. E.; Gilles, R. W.; Greene, N.; Huang, E.; Krieger-Burke, T.; Loesel, J.; Wager, T.; Whiteley, L.; Zhang, Y., Physiochemical drug properties associated with in vivo toxicological outcomes. Bio*org Med Chem Lett* **2008, 18** (17), 4872-5.

43. Arnott, J. A.; Planey, S. L., The influence of lipophilicity in drug discovery and design. E*xpert Opin Drug Discov* **2012, 7** (10), 863-75.

44. For a similar transformation involving a cyclobuntane nitrile, see: Lemieux, R. M. et al(2009) Patent Cooperation Treaty Int Appl WO 2009070485.

Insert Table of Contents artwork here

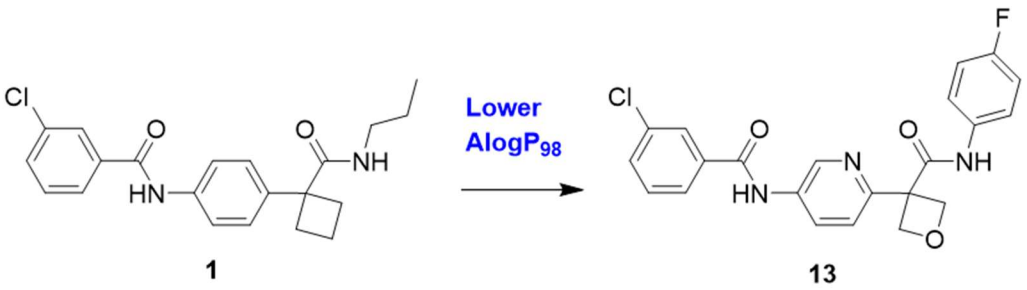

	1	13
IDO1 HeLa IC_{50}	9 nM	3.2 nM
IDO1 hWB_u IC_{50}	22 nM	0.6 nM
$AlogP_{98}$	4.4	3.1
FASSIF Soly (µM) pH 6.5	58	170
Rat *in vivo* Cl_{int} (ml/min/kg), Vd_u (L/kg), MRT(h)	>Qhep, 180, 0.7	590, 99, 3.2